Friction Dynamics In Mechanical Bar Spreading For Unidirectional Thin-Ply Carbon Fiber

ul-Haq, Ehshan; Hondekyn, Marie; Yuksel, Onur; Dransfeld, Clemens; Caglar, Baris

Publication date
2024

Document Version
Final published version

Published in
Proceedings of the 21st European Conference on Composite Materials

Citation (APA)
ul-Haq, E., Hondekyn, M., Yuksel, O., Dransfeld, C., & Caglar, B. (2024). Friction Dynamics In Mechanical Bar Spreading For Unidirectional Thin-Ply Carbon Fiber. In C. Binetury, & F. Jacquemin (Eds.), *Proceedings of the 21st European Conference on Composite Materials: Volume 5 - Manufacturing* (Vol. 5, pp. 399-406). The European Society for Composite Materials (ESCM) and the Ecole Centrale de Nantes..

FRICTION DYNAMICS IN MECHANICAL BAR SPREADING FOR UNIDIRECTIONAL THIN-PLY CARBON FIBER

Ehshan ul-Haq[1], Marie Hondekyn[2], Onur Yuksel[1], Clemens Dransfeld[1] and Baris Caglar[1]

[1]Aerospace Structures and Materials Department, Faculty of Aerospace Engineering, Delft University of Technology, Kluyverweg 1, Delft 2629HS, the Netherlands
[2]Mechanics of Materials and Structures, Department of Materials, Textiles and Chemical Engineering, Ghent University, Technologiepark 46, Zwijnaarde 9052, Belgium

Email first author: E.ul-Haq@tudelft.nl

Keywords: carbon fiber, composites, tow spreading, unidirectional, thin-ply

Abstract
Thin-ply carbon fiber reinforced polymers (CFRP) have claimed significant attention for their potential to surpass traditional composite materials in terms of performance metrics such as first-ply damage criteria, fatigue life, and ultimate strength. This study focuses on investigating the friction behavior of dry carbon fiber tow during mechanical bar spreading, a crucial process in the manufacturing of thin-ply CFRP. By systematically examining the interplay of wrap angle, tow pre-tension, and final tension, insights are provided into the frictional forces exerted on the carbon fibers. The study utilizes an experimental framework to analyze single-bar and multi-bar setups, considering both symmetric and asymmetric configurations. Results reveal non-linear friction behavior, with increasing wrap angles leading to decreased dynamic friction coefficients. Additionally, results seem to suggest that higher pre-tension reduces internal tow movement, thereby decreasing friction losses. Multi-bar setups exhibit distinct friction profiles compared to single-bar setups, especially for larger wrap angles and asymmetric cases, indicating the influence of superimposed wrap angles on friction. Recommendations for future research include further exploration of factors such as non-uniform normal loads and relaxation distances between spreader bars to enhance modeling accuracy and optimize friction performance.

1. Introduction

Thin-ply carbon fiber reinforced polymers (CFRP) offer a promising pathway to overcome the limitations of traditional composite materials, delivering improvements in first-ply / first-damage criteria, fatigue life, and ultimate strength [1]. Typically characterized by individual plies with a thickness below 0.1mm, these composites leverage size effects and design flexibility, facilitating smaller pitch angles at specific thicknesses [2,3,4].

Diverse techniques for producing unidirectional thin plies include airflow spreading, ultrasonic vibration, and mechanical methods [5]. Mechanical bar tow spreading, a method involving controlled tension to pull dry tows through bars or pins, is the considered method for spreading in the context of this study.

This work introduces an experimental framework to systematically assess and quantify the influence of various mechanisms on the friction behavior of dry carbon fiber tow during mechanical bar spreading. By examining the interplay of wrap angle, tow pre-tension, and final tension, the objective is to provide valuable insights into the friction behavior of carbon fibers in mechanical spreading processes and to what extent the friction behavior correlates with established expressions [6]. The frictional forces exerted on the carbon fibers can lead to damage, besides geometrical alterations, which may compromise

the composite material's structural integrity and mechanical properties. Understanding and mitigating such damage mechanisms is crucial for optimizing the mechanical spreading process and enhancing the overall performance of thin-ply composites.

The subsequent sections provide an overview of bar spreading mechanics, detail the methodology employed in the experimental framework, present and discuss the results obtained, and conclude with implications and future directions for research in this area.

1.1. Mechanics of bar tow spreading

Several forces play a role in the tow spreading process: tension within the filaments, friction between the filaments, and friction between the filaments and the spreading bar. When a fiber bundle is tensioned around a spreader bar, the normal components of tension, perpendicular to the fiber direction, drive upper filaments into the gaps between the filaments beneath. Filaments further from the bar surface experience greater strain and tension due to the increased radius, making them more prone to downward movement and push the fibers closer to the bar that in turn results in spreading. As they descend, strain decreases and tension lessens, countered by fiber-fiber friction [7]. Due to the tow motion over the metal spreader bar, fiber-metal Coulomb friction occurs. The friction results in a normal force N on the roving, causing the fibers to undergo spreading. Considerations include increased fiber-bar contact and lateral strain, which limits spreading. The interplay between tension and friction profoundly influences the tow's spreading behavior [8].

The role of friction isn't confined to spreading; it also leads to material damage through mechanical material-to-material interaction [7]. It is crucial to note that the damage inflicted on the roving material can impact the final part's performance, as it is not mitigated during further stages of manufacturing processes. For this reason, it is important to have a comprehensive understanding of the friction behavior of the material. This study reports an experimental approach on determining the influence of several process parameters in the force buildup in the fiber spreading process and thus the friction.

1.2. Capstan equation and alterations

The friction between the fiber tow and the cylindrical spreading bar, also named a 'Capstan', occurs at their interface. In friction mechanics, the Capstan equation (Eq. 1) is employed to analyze friction in a setup where a belt is wound around a cylinder. The Capstan equation provides a fundamental relationship describing the tensile force, T_2, exerted on one side of the belt when a tensile force, T_1, is applied on the other side. A simplification is made by Gupta to simplify the fibrous roving to a belt structure, assuming the Capstan is rigid and the belt structure is simplified to a one-dimensional object [9]. These assumptions enable the derivation of a simplified equation describing the relationship between the applied force and the resulting tension in the belt, facilitating the analysis of friction in the system.

$$T_2 / T_1 = e^{\mu\phi}. \tag{1}$$

for which μ is the apparent friction coefficient where $\mu = F / N$ and ϕ is the total wrap angle of the tow around the Capstan in radians.

The above-mentioned equation (Eq. 1) assumes a direct proportionality between the friction force F and the normal force N [9]. Other works assume a non-linear correlation, as is displayed below in Equation 2 [10].

$$F = aN^n. \tag{2}$$

for which a is an experimentally determined proportionality constant which relates the normal force N with the friction force F, similar to μ in Eq. 1, and n is a fitting parameter with $n < 1$. The value of n

refers to the deformation mechanics of the system and it is considered that $n = 1$ for fully plastic deformation and $n = 2/3$ for fully elastic deformation [8].

This correlation can be further supported by the adhesion theory of Bowden and Tabo [10]. For this, it is claimed that the surface bonding effect is caused by shear friction events at certain points of mechanical contact. This can be written as

$$F = \tau A. \tag{3}$$

for which τ is the shear strength of the junction and A is the real contact area between objects.

For many materials there is an apparent linear correlation between the real contact area A and the applied normal load N. However, it was observed that, for some materials, there is no linear correlation to be noted between the real contact area and the applied normal load [10].

A new expression for the Capstan equation was derived by Howell, using the above-mentioned Equations 2 and 3, and is displayed in Equation 4 [9].

$$T_2 / T_1 = e^{a\phi(r/T1)\hat{}(1-n)}. \tag{4}$$

for which a and n are fitting parameters similar as discussed for Equation 2 and r is radius of the cylinder (Capstan). It should be noted that the tension ratio T_2 / T_1 is now expressed as a function of pre-tension T_1. Other works have incorporated this non-linear interaction of the materials and built hereon [11].

2. Methodology

This study aims to establish a comprehensive framework for evaluating the characteristics of dry carbon fiber rovings and leveraging it to monitor and predict the behavior of carbon fiber rovings during mechanical bar spreading. An experimental setup, allowing single-bar and multi-bar spreading configurations, was used for collecting data at various process conditions. The findings were subsequently compared with Howell's solution, including pre-tension and radius dependency, listed in the previous section.

2.1. Framework for assessment of mechanical bar tow spreading

For assessing the friction behavior of dry carbon fiber rovings in the mechanical spreading process, a systematic approach of measurements was followed. This approach consisted of pulling Toray T700SC 12K dry carbon rovings through bar(s) placed in various configurations while monitoring the resulting system friction by using a pair of calibrated tension sensors placed before and after the spreader bars. A subdivision was made into single-bar friction events and multi-bar friction events, for which cases from 1 to 4 bars were selected for this study. By employing various bar configurations, including similar wrap angles superimposed over multiple bars, an inventory of wrap angles and tension values was collected. Studied configurations were then analyzed for their friction properties and fitted using Equation 4. Any deviations from this, or similar models, can potentially be explained or improved upon. Table 1 shows the experimental bar setups for the proposed study.

Table 1. Experimental matrix of various spreader bar configurations.

Experiment type	Total wrap angle ϕ (°)	Bar count	Wrap angle ϕ (°) division
Single bar	*40, 60, 120, 160*	*1*	*40, 60, 120, 160*
Multiple bars, symmetric	*80, 160, 160*	*2, 4*	*40* x*2, 40* x*4, 80* x*2*
Multiple bars, asymmetric	*160, 160*	*2*	*120+40, 40+120*

Pre-tension values were varied using a mechanical brake during unwinding, set to 20%, 60%, and 100% braking power. Relative velocity was fixed for this study at 4.6m/min. Each setup run was performed 3 separate times for verification. Below in Figure 1, a diagram is shown of the setup.

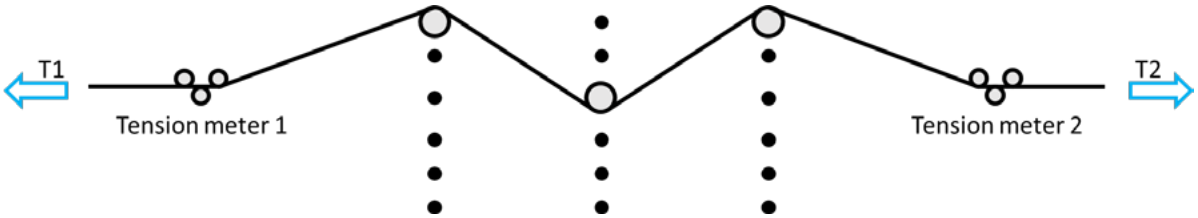

Figure 1. Example setup diagram for multi-bar experiments. Case shown for a 3-bar setup.

An analysis was performed on the friction behavior for various configurations of spreader bars. To obtain a mathematical expression of the friction behavior, of a tow passing through an m-number of bars at various angles ϕ_m, Equation 4 was modified to obtain Equation 5 below.

$$T_{final} / T_{start} = {}_{m=1}\prod^{m} (e^{\ a\phi m(r/Tm)\hat{}(1-n)}) \tag{5}$$

where T_{start} refers to the incoming global tension, T_{final} refers to the outgoing global tension, and T_m refers to the local pre-tension before each spreader bar which changes for each interaction with $\phi > 0^o$.

2.2. Experimental setup

Figure 2 shows the setup used in this study, that can unspool dry carbon roving with a controlled tension force through adjustable mechanical spreader bars. The bars are manually adjustable over a broad range of wrap angles, with the potential to reach a wrap angle up to 180º per bar with 4 bars installed. The bars have a diameter of 15mm and are finished with a topochrome coating. A pulling assembly featuring 5 pulling axles and chain drive, powered by a 24V DC motor, delivers the required pulling force. Tension sensors are installed before the first bar and after the last bar and they are connected to a National Instruments 6009. The setup is powered by a 720W PSU and is controlled via an Arduino Uno in combination with custom code for driving, capturing and analysis.

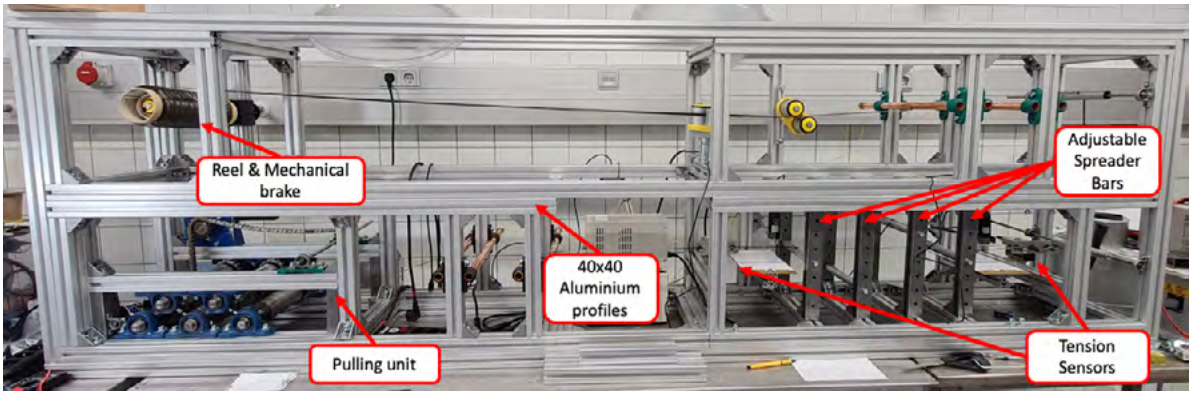

Figure 2. Experimental tow spreading setup with tags.

3. Results and discussions

In this section, the results are displayed and discussed. These outcomes are analyzed according to Howell's friction model which takes pre-tension T_1 into account (Eq. 4) and fitting parameters are shown. This section is subdivided into single-bar and multi-bar experiments.

3.1. Single-bar cases and friction behavior

Figures 3a and 3b show both the tension ratio T_2 / T_1 as the resulting apparent friction coefficient μ for single-bar setups featuring 40º, 80º, 120º, and 160º wrap angles where each datapoint corresponds to an average of 3 seconds of real-time measurement data. Figure 3c reports percentual width increases, measured with calipers both 10cm before the first spreader bar and 10cm after the last spreader bar for each run. Each point, per wrap angle, represents the average of 3 separate measurements.

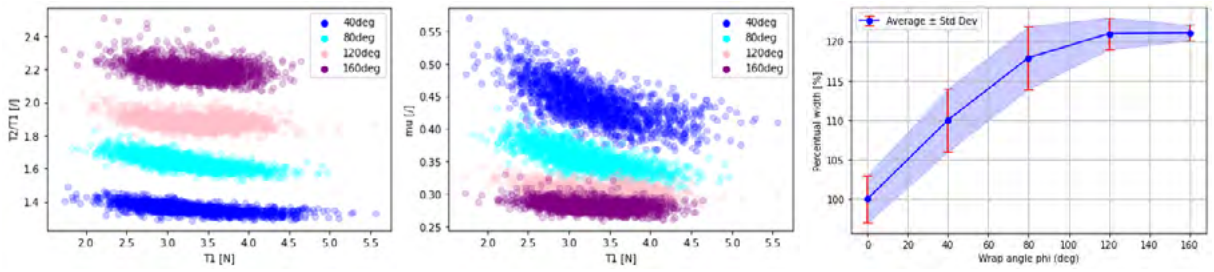

a **b** **c**

Figure 3. Tension ratio T_2 / T_1 vs pre-tension T_1 for various wrap angles ϕ (**a**). Apparent friction coefficient μ vs pre-tension T_1 for various wrap angles ϕ (**b**). Measured average roving width (off-bar) increase [%] for various wrap angles ϕ inc. standard deviation (**c**).

The incremental increase in wrap angle ϕ of 40º up to 160º leads to an increase in average tension ratio, and therefore a logarithmic decrease in apparent dynamic friction coefficient μ, as per Equation 1, or *a(r/T1)^(1-n)*, as per Equation 4. This is a first indication of non-linear friction behavior, where geometrical differences between friction events influence the measured dynamic friction coefficient. Also, the increase in wrap angle ϕ appears to result in an increased variability in the measured tension ratio T_2 / T_1. It is hypothesized that this correlation is due to larger wrap angles resulting in more points of physical interaction, which naturally increases variability. Lastly, all data groups show a negative trend with increasing pre-tension; as pre-tension T_1 is increased on the x-axis, a notable decreasing trend is visible in Figures 3a and 3b. This highlights the influence of pre-tension on the friction and spreading behavior.

The results were fitted to Equation 4 to quantify the measured non-linear behavior. A grid search optimization approach was employed to determine optimal parameter values for a and n, where the mean-squared-error was minimized. Fitting parameters a and n were noted per setup and are displayed in Table 2. Both Figure 3b and Table 2 show that the slope, represented by fitting parameter a, is decreasing over increasing pre-tension T_1. It is hypothesized that, as the carbon tow undergoes higher pre-tension, it approaches belt-like behavior. This could be due to the increased internal tow friction as well as the loading of the fibers, both reducing possible movements. As these internal movements are reduced, internal friction losses are reduced. This is visible by the global downward trends of the tension ratios in Figure 3a, which seems to approach an asymptote over increasing pre-tension, possibly explained by a maximum limit at which the structure would fully act as a belt-like object. It can also be seen from Table 1 that the parameter n increases both with wrap angle ϕ and pre-tension T_1. This indicates that the friction behavior tends to migrate towards a more linear regime under these higher-friction circumstances, as $n \rightarrow 1$.

Figure 3c displays the percentual width increase per wrap angle. A strong asymptotic behavior is visible. It must be noted that this asymptotic behavior might be a symptom of increased post-tension for higher wrap angles as the width is measured off-bar. As the exit tension increases, the fibers are held together to a higher degree, possibly limiting spreading capabilities. It is visible that the increase in spread from 80º upwards is relatively low, while the total friction does increase significantly as seen in Fig. 3a. This supports the suspicion that excess friction damages the material beyond requirements.

Table 2. Parameters *a* and *n* fitted for single-bar setup configurations.

Wrap angle ϕ (°)	T_1 = 20%	T_1 = 60%	T_1 = 100%	T_1 = 20%	T_1 = 60%	T_1 = 100%
	a	***a***	***a***	***n***	***n***	***n***
40	2.23	1.63	1.46	0.71	0.76	0.79
80	1.12	0.93	0.90	0.80	0.83	0.83
120	0.69	0.59	0.63	0.85	0.88	0.88
160	0.49	0.49	0.42	0.90	0.90	0.94

3.2. Multi-bar cases and superposition

In this section, an overview of the friction behavior is presented for various symmetric and asymmetric multi-bar tow spreading configurations. Table 2 displays the fitted parameters *a* and *n* according to Eq. 4 obtained through a grid search and minimization of the objective function. Figure 4 shows the experimental results.

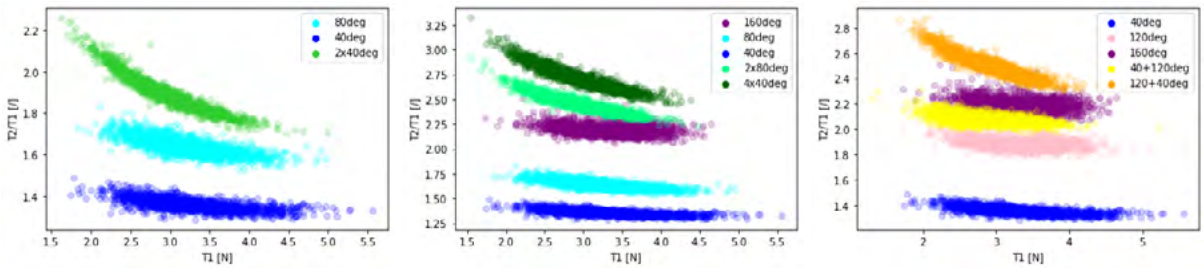

a **b** **c**

Figure 4. Tension ratio T_2 / T_1 vs pre-tension T_1 for wrap angles ϕ = 40°, 2x40, and 80º (**a**). Tension ratio T_2 / T_1 vs pre-tension T_1 inc. wrap angles ϕ = 80°, 2x80°, and 160º (**b**). Tension ratio T_2 / T_1 vs pre-tension T_1 inc. wrap angles ϕ = 40º+120º, and 120º+40º (**c**).

It can be seen in Figure 4 and Table 3 that theoretically similar scenarios (according to Eq. 5), yielding the same total wrap angle ϕ, show notably different friction behavior indicating different friction profiles. This indicates that the friction profile, per interaction, is not solely expressed by the wrap angle ϕ itself. In addition, for all measured symmetric cases, the superposition of wrap angles results in greater friction compared to single-bar cases with identical wrap angles. It is thought that the act of spreading corresponds to a great amount of friction. If a single bar is used, this spreading is relatively consistent over the bar surface. However, if that same wrap angle is divided over multiple bars, it is observed that the tow can reshape partially back to the original geometry between the spreader bars in the so-called relaxation distance. This is due to the axial tension that the tow undergoes between the various bars. The second interaction then has to 're-spread' some of the tow, hypothesized to explain the additional energy consumption.

Table 3. Parameters *a* and *n* fitted for multi-bar setup configurations.

Wrap angle ϕ (°)	T_1 = 20%	T_1 = 60%	T_1 = 100%	T_1 = 20%	T_1 = 60%	T_1 = 100%
	a	***a***	***a***	***n***	***n***	***n***
40 x*2*	4.07	4.00	3.44	0.60	0.60	0.63
40 x*4*	1.43	1.34	1.27	0.75	0.76	0.77
80 x*2*	1.31	1.26	1.16	0.74	0.75	0.76
40+120	0.55	0.52	0.46	0.86	0.88	0.90
120+40	1.37	1.24	1.18	0.74	0.76	0.76

It is also worth noting that when friction is increased, by increasing the wrap angle or pre-tension, the visible differences between setups becomes less noticeable and the friction behavior becomes more stable. This can be explained according to the geometrical properties of the carbon tow: as tension in the tow increases, the tow behaves more like a belt-like object as expressed by Eq. 1. Eventually, increased tension seems to reach a limit. This is supported by Figure 3c, where the width of a tow approaches a plateau for single-bar spreading as friction increases.

From the asymmetric results of Fig. 4c, displayed via yellow and orange scatterplots, it can be seen that pre-tension dependency is very present. Interestingly, the asymmetric cases perform differently compared to the single-bar identical wrap angle of ϕ = 160º. From Fig. 4c and Table 3 it is visible that the case of ϕ = 40º + 120º results in a lower final tension than the single ϕ = 160º, opposite of the ϕ = 120º + 40º case which results in higher final tension than the single ϕ = 160º. This confirms the non-linear behavior, earlier expressed as the fitting parameters a and n, and indicates that the sequence at which friction events are undergone influences the measured process properties.

Using single-bar measurement data, predictions were made for the multi-bar cases with the help of Eq. 5, displayed in Fig. 5. This is done to illustrate the existing deviations between superimposed bar setups, where direct comparisons are shown between measured data of both ϕ = 40º x2 and ϕ = 80º x2 to their predictions based on the single-bar measurements of ϕ = 40º and ϕ = 80º. As Fig. 5 displays, differences are visible in both cases. However, the 40º x2 prediction has a large overlap area suggesting that small wrap angles can be superimposed. This is further supported by the fitted curves in Fig. 5a, where the predictive fit for 2x 40º, based on the averaged fitting parameters for a single-bar case of 1x 40º from Table 2, and Eq. 5, aligns partially with the fitted curve directly obtained from the double-bar case from Table 3 of 2x 40º (also using averaged fitting parameter values). This is lesser the case for the scenario of 2x 80º within this experimental range.

The noted differences are expected to be due to the variations in superimposed bar setups mentioned above. Please note that, for both predictive results of Fig. 5, the extended portions of the linear data tails are a result of the calculation method and should be disregarded for analysis. Several aspects were not considered in the processing of this data of which some have been mentioned above. For future works, it could be beneficial in modeling accuracy to assess their influence in the spreading of carbon tow. These aspects are:

1. Non-uniform normal loads between tow and spreader bar
2. Variation of the relaxation distance between spreader bars
3. Over/under vs. over/over tow-bar interactions

These items are expected to have some effect on the measured friction behavior and can be mentioned to partially explain offsets in predictions and measurements.

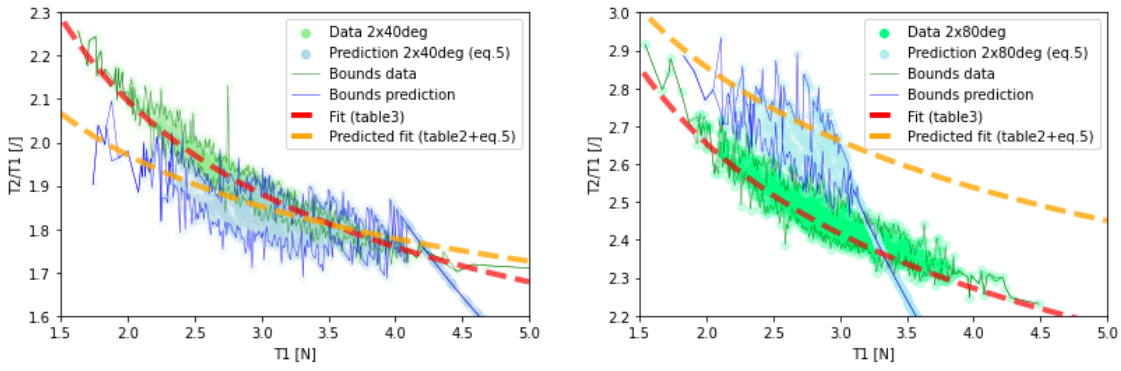

a **b**

Figure 5. Superimposed ϕ = 2x40º vs. predicted ϕ = 2x40º derived from single-bar (1x40º) measurements. (**a**). Superimposed ϕ = 2x80º vs. predicted ϕ = 2x80º derived from single-bar (1x80º) measurements (**b**). Fits (Table 3) and predicted fits (Table 2 + Eq. 5) are presented.

4. Conclusions and recommendations

This study examined the friction behavior during spreading of carbon fiber tows using single-bar and multi-bar setups, with a variation in wrap angle ϕ and pre-tension T_1. The results indicate non-linear friction behavior, with increasing wrap angles leading to a non-linear decrease in apparent dynamic friction coefficient. Moreover, increased pretensions appear to reduce internal tow movement, resulting in decreased friction losses, per area, hence decreased friction coefficients. Multi-bar setups exhibited different friction profiles compared to single-bar setups, with superimposing of wrap angles changing friction profiles. This behavior is dependent on the total wrap angle ϕ with minimal differences for low wrap angles. Asymmetric setups showed distinct behavior, suggesting that the sequence of friction events influences process properties. However, certain aspects such as relaxation distances between spreader bars and over/under bar configurations were not fully considered and could impact analysis accuracy.

Recommendations for future research include further investigation into influencing factors such as relative velocity, fiber types and their microstructures [12], relaxation distance, and over/under configurations, while exploring different tow-bar interactions may provide insights into optimizing friction performance. These recommendations aim to refine friction modeling, enhance the efficiency of carbon tow spreading processes, and aim to describe its correlations between spread width, applied damage, and measured friction.

References

[1] Amacher, R. et al. "Thin ply composites: Experimental characterization and modeling of size-effects." *Composites Science and Technology*, 101:121-132, 2014.
[2] Arteiro, A. et al. "Thin-ply polymer composite materials: A review." *Composites Part A: Applied Science and Manufacturing*, 132, 105777, 2020.
[3] Galos, J. "Thin-ply composite laminates: a review." *Composite Structures*, 236, 111920, 2020.
[4] Mencattelli, L. and Pinho, S.T. "Ultra-thin-ply CFRP Bouligand bio-inspired structures with enhanced load-bearing capacity, delayed catastrophic failure and high energy dissipation capability." *Composites Part A: Applied Science and Manufacturing*, 129, 2020.
[5] Arrabiyeh, P.A. et al. "An overview on current manufacturing technologies: Processing continuous rovings impregnated with thermoset resin." *Polymer Composites*, 42(11), 5630-5655, 2021.
[6] Cornelissen, B. "The role of friction in tow mechanics." PhD Thesis, *University of Twente*, 2013.
[7] Irfan, M.S., Machavaram, V.R., Mahendran, R.S., Shotton-Gale, N., Wait, C.F., Paget, M.A., Hudson, M. & Fernando, G.F. "Lateral spreading of a fiber bundle via mechanical means." *Journal of Composite Materials*, 311 – 322, 2012.
[8] Cornelissen, B., Rietman, B., & Akkerman, R. "Frictional behaviour of high performance fibrous tows: Friction experiments." *Composites Part A: Applied Science and Manufacturing*, 44, 95 – 104, 2013.
[9] Gupta, B., Ajayi, J., & Kutsenko, M. "Experimental methods for analyzing friction in textiles." *Friction in Textile Materials*, 174–221, 2008.
[10] Mulvihill, D.M., Smerdova, O., & Sutcliffe, M.P. "Friction of carbon fibre tows." *Composites Part A: Applied Science and Manufacturing*, 93, 185–198, 2017.
[11] Jung, J.H., Pan, N., & Kang, T.J. "Capstan equation including bending rigidity and non-linear frictional behavior." *Mechanism and Machine Theory*, 43(6), 661–675, 2008.
[12] Gomarasca S., Peeters D., Atli-Veltin B., Dransfeld C. "Characterising microstructural organisation in unidirectional composites." *Composites Science and Technology*, Volume 215, 2021.